Relaxometry and Magnetometry of Ferritin

Rodney A. Brooks, Josef Vymazal, Ron B. Goldfarb, Jeff W. M. Bulte, Philip Aisen

By combining nuclear magnetic relaxometry on 39 ferritin samples with different iron loading with magnetometry, results were obtained that suggest a new interpretation of the core structure and magnetic properties of ferritin. These studies provide evidence that, contrary to most earlier reports, the ferritin core is antiferromagnetic (AFM) *even at body temperature* and possesses a superparamagnetic (SPM) moment due to incomplete cancellation of antiparallel sublattices, as predicted by Néel's theory. This moment also provides a likely explanation for the anomalous T_2 shortening in ferritin solution. However, the number of SPM moments derived from this model is less than the number of ferritin molecules determined chemically, and a similar discrepancy was found by retrospectively fitting previously published magnetometry data. In other words, only a fraction of the ferritin molecules seem to be SPM. The studies also provide evidence for paramagnetic (PM) Curie-Weiss iron ions at the core surface, where the local Néel temperature is lower; these ions are apparently responsible for the weaker T_1 shortening. In fact, the conversion of uncompensated AFM lattice ions to PM ions could explain the small number of SPM particles. The apparent Curie Law behavior of ferritin thus appears to be a coincidental result of different temperature dependences of the PM and SPM components.

Key words: ferritin; superparamagnetism; T_1; T_2; relaxometry.

INTRODUCTION

Ferritin is nature's ubiquitous iron-storage molecule, found in species ranging from microbes to man. It consists of a roughly spherical protein shell called apoferritin (molecular weight = 450,000 kD), inside which iron accumulates in the form of a ferric oxyhydroxide crystal. The outer diameter is 12 nm, irrespective of the amount of iron stored within. Although its physical, chemical, and magnetic properties have been studied for more than 50 years, ferritin remains a subject of current research (1–8), with many implications for biology and medicine (9–14). In particular, ferritin is an important contributor to T_1 and T_2 relaxation, which effectively determine image contrast in MRI (15).

By combining nuclear magnetic relaxation studies and magnetization measurements, we have obtained a number of unexpected results that question some long-held beliefs.

MRM 40:227–235 (1998)

From the Neuroimaging Branch, NINDS (R.A.B., J.V.), and the Laboratory of Diagnostic Radiology Research, CC (J.W.M.B.), National Institutes of Health, Bethesda, Maryland; the National Institute of Standards and Technology, Boulder, Colorado (R.B.G.); and Albert Einstein Medical College, Bronx, New York (P.A.).

Address correspondence to: Rodney A. Brooks, Ph.D., Building 10, Room 5N214, National Institutes of Health, Bethesda, MD 20892.

Received July 10, 1997; revised January 27, 1998; accepted January 29, 1998.

Present address (J.V.): Department of Stereotactic and Radiation Neurosurgery, Hospital Na Homolee, Prague 5, 15119, The Czech Republic.

P.A. was partially supported by Grant DK15056 from the National Institutes of Health, U.S. Public Health Service.

SAMPLE PREPARATION

Thirty-seven ferritin samples with loading factor LF = 50–3400 were prepared in buffer (0.05 M MES, 0.1 M KCl, pH 6.5) by slow aerobic addition of ferrous iron to horse spleen apoferritin (33 samples; Sigma, St. Louis, MO) and ferritin (four samples; Boehringer Mannheim, Indianapolis, IN). The samples were allowed to oxidize by ambient dioxygen, with deposition of resulting Fe^{3+} on the growing ferric oxyhydroxide core. Samples of unprocessed Sigma ferritin (LF = 1900) and unprocessed Boehringer ferritin (LF = 2740) were also included. Except for one batch of 17 Sigma samples, centrifugation was performed to remove small precipitates that formed at the higher loading factors. Weakly bound and extraneous iron was minimized by passage through a column of chelating resin (Chelex 100, BioRad, Hercules, CA), and the preparations were concentrated by ultrafiltration to protein concentrations of 5–15 mg/ml. Final concentrations of iron and protein were measured by a FerroZine-based assay (Aldrich Chemical Co., Milwaukee, WI) and a modified Lowry method (16), respectively, and the loading factors were calculated.

RELAXOMETRY

Background

Nuclear magnetic relaxometry is a powerful tool for studying paramagnetic (PM) and superparamagnetic (SPM) particles by observing their effect on the nuclear magnetic relaxation times T_1 and T_2 of solvent water protons as a function of magnetic field H (or, equivalently, Larmor frequency f). In the first such study of ferritin in solution, it was stated that the iron core has no effect on T_1 (17), but this finding was later contradicted (18). A strong T_2 effect was also seen (17–20), with an anomalous linear dependence on magnetic field (18, 19) and an uncertain dependence on LF (18, 20).

Methods

T_1 and T_2 were measured with a variable-field relaxometer (19) at magnetic fields H = 0.025–1.5 T (f = 1–64 MHz) and temperatures T = 3°, 23°, and 37°C. T_1 was determined from 32 saturation recovery sequences, and T_2 was determined from a CPMG sequence of 100–500 spin echoes with 2-ms interecho time. Reciprocals were taken, buffer values were subtracted, and the results were divided by the mM ferritin concentration to obtain T_1 and T_2 relaxivities (s^{-1}/mM protein).

Results

In Fig. 1, the T_1 relaxivity is plotted versus LF at 37°C and 1 T. Previously published results (18, 19) are included (after multiplying by 9 to convert to the present units). The data sets at each temperature and field were fitted

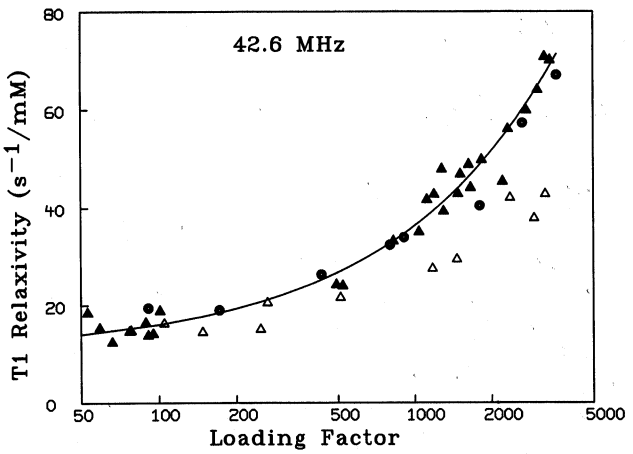

FIG. 1. Semilogarithmic plot of T_1 relaxivity at 1 T and 37°C. Present results (triangles) are shown along with previously published data (circles) (18, 19). The solid line is an empirical fit using Eq. [1], omitting uncentrifuged samples with $LF > 100$ (open triangles). Note: The curvature, which is concave upward here, would be concave downward on a linear plot.

with the empirical function

$$1/T_1 = A + B\ LF^{\beta} \qquad [1]$$

Outliers were omitted from the fitting, including 10 uncentrifuged samples with $LF > 100$ and the unprocessed Sigma sample. Fitted parameters for the data of Fig. 1 are $A = 11.3$, $B = 0.231$, and $\beta = 0.67$. T_1 data at other fields and temperatures were sometimes more variable, and a three-parameter fit was not always meaningful; however, a reasonably good fit of all data was obtained by fixing β at 0.67 (estimated uncertainty ± 5%). The resulting values of A and B are shown in Fig. 2.

The behavior of $1/T_2$ is different; it becomes much larger than $1/T_1$ for LF > 100, and its dependence on frequency is consistently linear. Thus, the $1/T_2$ data can be summarized by presenting the $1/T_2$ vs. f slopes, as in Fig. 3. Again, previously published data are included. Note that the T_2 outliers are from a different batch than the T_1 outliers. If this batch is omitted from the fitting, we find that the slopes are approximately proportional to LF, with coefficients 0.0048 (s^{-1}/mM)/MHz at 37°C (solid line in Fig. 3), 0.0060 (s^{-1}/mM)/MHz at 23°C, and 0.0083 at 3°C.

Discussion

T_1

The value $\beta = 0.67$ is somewhat less than the 0.75 value suggested earlier (18), but it is based on more than 2000 T_1 measurements on 39 samples versus fewer than 100 measurements. From the standpoint of using MRI measurements of T_1 to help determine tissue iron content (8), a linear relationship would have been preferable since, for a given amount of iron, T_1 would then be independent of LF. However the $LF^{2/3}$ dependence may not present problems if the range of LF *in vivo* is not too great.

The parameter A represents the value of $1/T_1$ extrapolated to $LF = 0$; i.e., it gives the contribution of apoferritin plus any noncore Fe ions that may be present. Indeed, the behavior of A (Fig. 2a) is virtually identical, in magnitude and frequency dependence, to $1/T_1$ for apoferritin with several bound Fe ions (17), and the downward temperature dependence is consistent with the decrease in viscosity at higher temperature.

The coefficient B represents the core contribution to $1/T_1$. It has a somewhat different frequency dependence than A (Fig. 2b), with a smaller dip followed by an increase for $f > 10$ MHz. Also, the temperature dependence is smaller, more variable, and generally in the opposite direction. Our initial attempts to explain this behavior with theories of relaxation by SPM moments (21, 22) were not successful. There are, however, a number of observations that suggest a PM origin. (a) The frequency dependence of B is similar to that of other PM ion-protein complexes (23, 24). (b) The magnitude of B (approximately 45 s^{-1}/mM for $LF = 3000$) is similar to the effect of approximately 15 Fe^{3+} ions bound to apoferritin (at pH 4.9) (17). (Although 15 is a reasonable number, it should not be taken literally, since the relaxation effect per ion may vary widely for different chemical sites.) (c) The small positive temperature dependence of B is consistent with exchange-limited "inner-sphere" PM relaxation. (d) The value $\beta = 0.67$ is consistent with a surface contribution, since the surface area of a regular solid is proportional to the two-thirds power of its volume. Thus, all observed properties of T_1 can be explained on the basis of inner-sphere relaxation by PM Fe^{3+} ions at the core surface.

T_2

An unusually short T_2 in the presence of magnetic particles is usually considered to be a microscopic susceptibility effect, caused by dephasing of water protons as they diffuse through field gradients created by the induced magnetization of the particles. Furthermore, the temperature dependence of T_2 is consistent with outer-sphere (i.e., diffusion) relaxation theory, because of the change in viscosity with temperature. Even the fact that different samples are T_1 and T_2 outliers (*cf.*, Figs. 1 and 3) is consistent with the concept of different relaxation mechanisms, i.e., T_1 is affected by external PM ions and T_2 by an SPM moment arising from the core structure.

However, the linear dependence of $1/T_2$ on frequency, seen only in solutions of ferritin (18, 19) and other ferric oxyhydroxide particles (25), is not consistent with standard relaxation theory, and the linear dependence on LF is similarly difficult to explain. (A quadratic dependence on LF was reported at 9.4 T (20), but it was based on only five data points and there was appreciable uncertainty in the fitting.) Now, according to Curie's Law, the average aligned magnetization of each particle increases linearly with applied field and quadratically with its magnetic moment μ_s. Thus, $1/T_2$, which is theoretically proportional to the square of the aligned magnetization, should be proportional to f^2 and to μ_s^4. But the former relationship is contrary to observation, and the latter implies $\mu_s \propto LF^{1/4}$, which is counterintuitive. However, if we accept as an empirical fact that $1/T_2$ depends *linearly* on the aligned magnetization (based on the observed linear dependence on f), then the dependence on μ_s is reduced

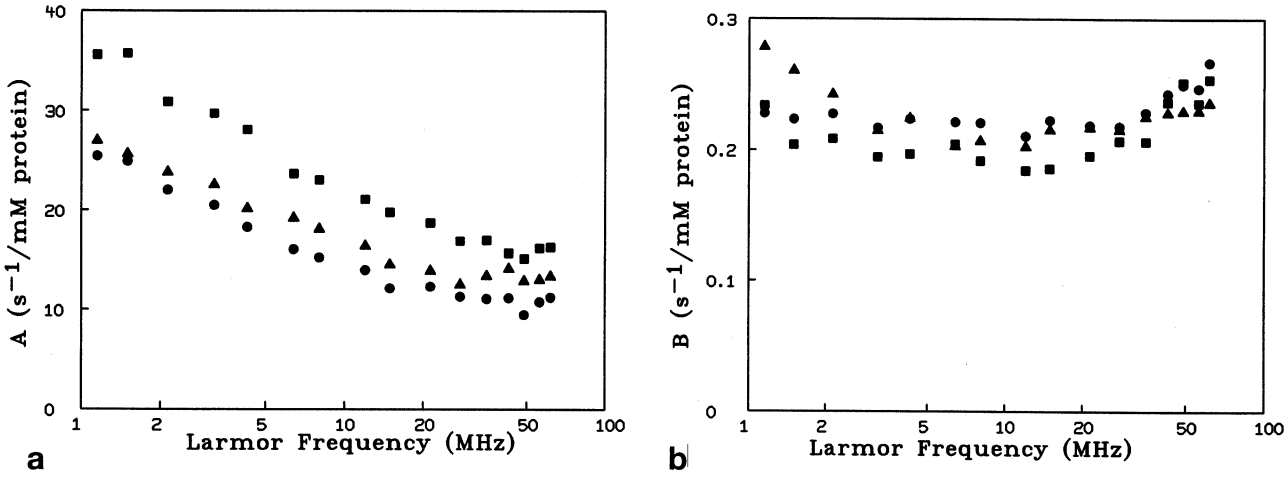

FIG. 2. (a) Fitted values of A ($1/T_1$ extrapolated to $LF = 0$) for temperatures of 3 (■), 23 (▲), and 37°C (●). (b) Similar plots of B (coefficient of the core contribution to $1/T_1$).

from μ_s^4 to μ_s^2 (18). This leads to $\mu_s \propto LF^{1/2}$, a relation (as we will see later) that is in accord with theory.

In summary, the magnitude of the core contribution to $1/T_2$, its dependence on loading factor, and its dependence on temperature are all consistent with the assumption that the ferritin molecules possess an SPM moment. The linear dependence on LF is favorable for the use of MRI in the quantification of tissue iron, since the T_2 effect of a given amount of iron is then not affected by variations in LF. The linear dependence of $1/T_2$ on f, however, remains to be explained.

MAGNETOMETRY

Background

Measurements of magnetization M versus field H were first performed on ferritin in solution at 3° and 23°C (26).

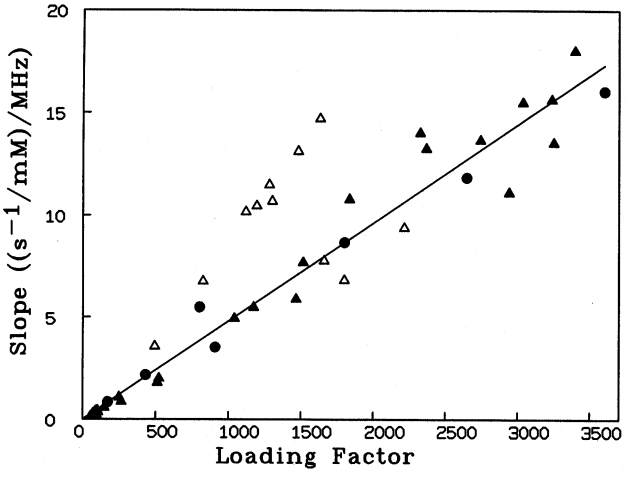

FIG. 3. Slopes of $1/T_2$ relaxivity vs. Larmor frequency at 37°C. Present results (triangles) are shown along with previously published data (circles) (18, 19). Note that the T_2 outliers are from a different batch (open triangles) than the T_1 outliers. The solid line shows a linear fit, with the outier batch omitted.

An apparent Curie Law behavior was seen, albeit with an atypical moment (for Fe^{3+}) of 3.8 Bohr Magnetons (BM); this was attributed at the time to an unusual electronic configuration. Subsequent measurements on lyophilized ferritin (27–32) showed that the Curie behavior at low fields extends down to 30 K, but at higher fields (and low temperatures), the M versus H curves display a concave downward curvature, followed by an asymptotic upward slope (28–32) (*cf.* Fig. 4). The curvature is indicative of an SPM moment approaching saturation[1] and was originally attributed to a ferromagnetic component of the ferritin core (28). The asymptotic slope, on the other hand, exhibits a temperature dependence (at least to 220 K) that is consistent with the Curie-Weiss (C-W) Law with a negative C-W constant[2] (28). Thus, the model of ferritin that emerged in 1965–1967 consisted of a ferromagnetic/SPM component that saturates at low temperatures and an antiferromagnetic (AFM) component that is above the Néel temperature and, hence, PM. However, this picture left a number of questions and inconsistencies, such as what happens at temperatures higher than 220 K.

Coincidentally, Néel, working in the field of rock crystals, had just shown that small AFM crystals can exhibit an SPM moment because of incomplete cancellation of

[1] An SPM particle has internal magnetic order (ferromagnetic, ferrimagnetic, or uncompensated antiferromagnetic) and, hence, a large magnetic moment compared to atomic or ionic moments. However, its size is so small that at most temperatures thermal energy exceeds magnetocrystalline and other anistotropy energies; thus, an ensemble of such particles behaves paramagnetically, according to the Langevin function. However, there is a "blocking temperature" below which the thermal energy is not sufficient to overcome the lattice forces and the particles, therefore, exhibit hysteresis and magnetic viscosity. The blocking temperature is a function of both time scale and field magnitude of the magnetic measurement, increasing for shorter measurement times and smaller fields.

[2] The Curie-Weiss Law (Eq. [7]) applies to ferro-, ferri-, or antiferromagnetic materials that are above the transition temperature and hence are spin-disordered. We refer to the component ions as "C-W PM ions" to distinguish them from PM ions that obey Curie's Law. For AFM materials, the transition temperature is known as the Néel point T_N, and the resulting C-W constant is negative. The magnetization of C-W ions, therefore, is less than that of Curie ions with the same moment, and the temperature dependence is more gradual.

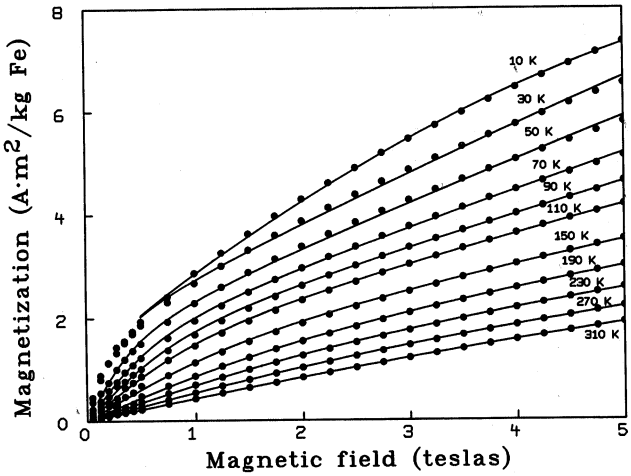

FIG. 4. Magnetization of ferritin powder per kg Fe (=emu/g Fe) plotted versus magnetic field for $LF = 3040$. Some data points are omitted at low fields, for clarity. Solid lines show the theoretical fits (see text).

AFM sublattices (33). For a crystal containing n paramagnetic ions with "saturation" moment μ_i, Néel estimated that there will generally be an excess of spin orientations in one direction or the other that results in a net magnetic moment

$$\mu_s = \mu_i n^{\alpha} \qquad [2]$$

where α lies between 1/3 and 2/3. Furthermore, if the crystal is small enough that the anisotropy energy is less than the thermal energy, the orientation of the spins will be unhindered by lattice constraints, and μ_s will be, by definition, superparamagnetic.[1] (Note, however, that the moment, although large compared with a single ion, is small compared with ferrimagnetic and ferromagnetic particles of similar size.)

Thus, Néel's theory offers an alternative explanation for the SPM moment of ferritin, especially considering that the core is known to be AFM at low temperature. The problem is that T_N of ferritin is not known, although various estimates have appeared in the literature, including 20 K (27), 174 K (34), and 240 K (35). However, the 20 K value is now known to result from a blocking temperature artifact, the 174 K estimate was made by extrapolating measurements of thermoremanence under the questionable assumption that the sample included "very small grains whose blocking temperature T_B must be very close to T_N," and the 240 K estimate was obtained by a rough extrapolation of Mössbauer data on an unrelated substance, concanavalin A. Whereas these published estimates led to a general belief that T_N is 240 K or lower, two recent reports have suggested, implicitly (31) and explicitly (32), that it may be much higher. A similar suggestion was made in a relaxometry study (18), in an attempt to explain the anomalous T_2 shortening that had previously been attributed to a ferromagnetic component (17). (It is interesting that the evolution of ideas in relaxometry paralleled the developments in magnetometry.)

Thus, the current view (30–32) is that the SPM moment of ferritin results from AFM order (33), while the linear component has been reinterpreted accordingly as arising from either bulk AFM susceptibility[3] (30) or "superantiferromagnetic" susceptibility[4] (31, 32). Note that the concept of two magnetization components, one SPM and one linear, has not changed—only the interpretations have changed.

Methods

A ferritin sample with $LF = 3040$ was lyophilized and sealed in a gelatin capsule. Its magnetization was then measured at temperatures from 10 to 310 K and magnetic fields from 0 to 5 T. Measurements were made with a commercial magnetometer based on a superconducting quantum interference device (SQUID). Results are expressed as $A \times m^2/kg$ Fe (= emu/g Fe). In addition, the low-field susceptibility was measured at temperatures extending down to 1.8 K.

Results

The M versus H curves are shown in Fig. 4. Careful examination shows that the curvature that is so striking at low temperature is also present at 310 K, indicating that SPM behavior is indeed present *at body temperature*. A slight secondary curvature can also be seen in the high-field region at 10 and 30 K. The susceptibility measured at 1.8 K was 3.81×10^{-6} m^3/kg Fe (= 3.03×10^{-4} emu/g Fe).

The data were first fitted with a Langevin function plus a linear susceptibility term (31, 32), but the "linear" term was later replaced with a Brillouin function in an attempt to fit the secondary curvature. This curvature is expected for PM materials, which may show incipient saturation at very low temperature, but not for bulk AFM susceptibility (36)[3]. Thus, the final fitting function (in SI units) was

$$M = N_p \mu_i B_S(\mu_i \mu_o H/(kT)) + N_s \mu_s L(\mu_S \mu_o H/(kT)), \qquad [3]$$

where

$$B_S(x) = (1 + 0.5/S)\coth[(1 + 0.5/S)x] - \coth[x/(2S)]/(2S) \qquad [4]$$

is the Brillouin function for PM ions with spin S (=5/2 for high-spin Fe^{3+}), and

$$L(x) = \coth(x) - 1/x \qquad [5]$$

[3] AFM susceptibility results from partial disruption of the antiparallel spin alignment by an applied magnetic field. If the field is perpendicular to the spin alignment, the susceptibility is a constant $\chi_\perp$ below T_N; if it is parallel, the susceptibility increases from 0 at 0 K to $\chi_\perp$ at T_N. For random alignment, the total susceptibility is the 2:1 weighted average of the two and, hence, increases from $0.67\chi_\perp$ at 0 K to $\chi_\perp$ at T_N (36).

[4] Néel has shown (37) that small AFM crystals with an even number of lattice planes (which therefore do not have an SPM moment) exhibit an enhanced AFM susceptibility called "superantiferromagnetism" if the field is perpendicular to the spin alignment. It is caused by a "couple . . . which tends to align the direction [of spin-alignment] locally along the direction of H . . . Hence the antiferromagnetic direction should turn progressively within the particle" (37). In a simple example (38), Néel found that "the susceptibility of these particles is twice as great as that of the corresponding bulk antiferromagnet" and that "the extra susceptibility . . . is already reduced by half for $T = 0.4\ T_N$." For randomly oriented crystals, two-thirds would exhibit this additional susceptibility, so the total susceptibility, instead of increasing with temperature, would actually decrease, from $1.33\ \chi_\perp$ at 0 K to $\chi_\perp$ at T_N.

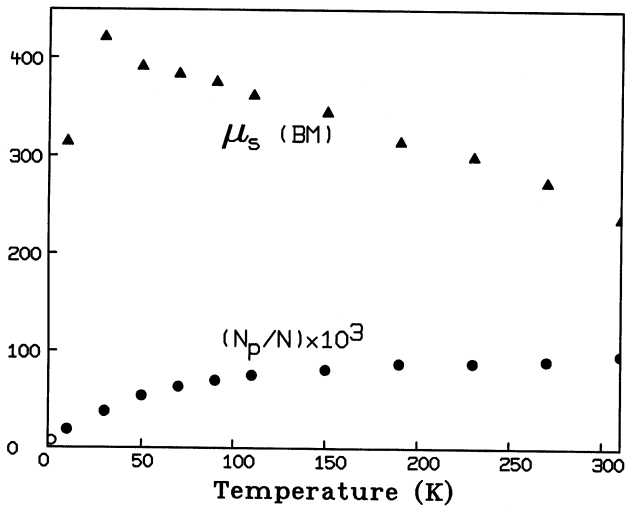

FIG. 5. Parameters obtained from the curve fits of Fig. 4. μ_S (▲) is the superparamagnetic moment in Bohr magnetons and N_p/N (●) is the fraction of PM Fe ions, assuming Curie Law behavior. The value of N_p/N obtained from the total susceptibility measurement at 1.8 K, assuming Curie behavior, is also shown (○).

is the Langevin function (the "classical" or high spin limit of B_S for S $\rightarrow \infty$). Other parameters are:

N_p = number of PM Fe^{3+} ions per kg Fe,
N_s = number of SPM particles per kg Fe,
μ_i = saturation magnetic moment of Fe^{3+} (5 BM)
μ_s = SPM moment
$\mu_o H$ = flux density in T,
k = Boltzmann's constant.

The Brillouin function is a generalization of Curie's Law and is effectively linear with field at temperatures higher than 30 K, with a built-in 1/T temperature dependence. However, since we do not know with certainty whether the origin of this term is PM or AFM susceptibility, we shall allow for the possibility of other temperature dependences by letting the coefficient N_p vary with temperature. Whereas Eq. [3] applies strictly to a homogeneous set of molecules, it should also be valid for reasonably narrow distributions.

The data at all temperatures were fitted *simultaneously* (MLAB, Civilized Software, Inc., Bethesda, MD) using Eq. [3] with variable parameters N_p, μ_s, and N_s, omitting data at 10 and 30 K because of concerns about hysteresis below the blocking temperature. N_s was assumed to be independent of temperature, under the assumption that the number of SPM particles is constant, but N_p was allowed to vary with temperature (see above). Using the value of N_s so determined, the 10 and 30 K data were then fitted, omitting points lower than 0.5 T (again because of hysteresis below the blocking temperature).

The results are shown in Fig. 4. The fits are generally good. In particular, the secondary high-field curvature at 10 and 30 K is fitted fairly well by the Brillouin function. The fitted value of N_s, expressed as a ratio to the total number of Fe atoms per kg ($N = 1.08 \times 10^{25}$), is $N_s/N = 4.62 \times 10^{-5}$ (estimated error ± 2.4%). Fitted values of μ_s and N_p/N are shown in Fig. 5 (estimated error ± 1–10%, depending on temperature); they are monotonically consistent for all temperatures higher than 30 K.

Discussion

SPM Component

The value of μ_s drops from approximately 400 BM at low temperature to 225 BM at 310 K. (Results at 10 and 30 K are not reliable because of blocking effects.) The low-temperature limit agrees with Néel's theory (Eq. [2]) with $\alpha = 0.54$, a value in the middle of his suggested range. This value of α is also in remarkably good agreement with the square root dependence of μ_s on *LF* suggested by the T_2 analysis above. Finally, the decrease with temperature is predicted by Néel's theory, because the ionic moment μ_i "decreases regularly from its saturation value . . . down to zero as the temperature increases from absolute zero to the Néel temperature" (33).

The value of N_s, however, is surprising. It corresponds to one SPM particle for each 21,600 Fe atoms—a much larger number than the chemically determined loading factor of 3,040. In other words, the number of SPM particles seems to be approximately one-seventh of the number of ferritin molecules—a result so unexpected as to suggest a possible flaw in the model or in the data; however, we have been unable to find such a flaw. This discrepancy is not just a subtle quirk in curve-fitting; the fit is clearly inadequate if N/N_s is constrained to the chemically determined ratio, as shown in Fig. 6. The reason this discrepancy has not been noted before is probably because in two studies (28, 29) curve-fitting was not done, whereas in the other three (30–32), the iron concentration was not given. In fact, by "retrofitting" the former two data sets with Eq. [3], we found a ratio of one SPM particle per 15,000 Fe atoms in each case—again, a much higher number than any possible loading factor. In addition, preliminary measurements on three other samples (unpublished data) resulted in similar discrepancies by a factor ranging from 4 to 8.

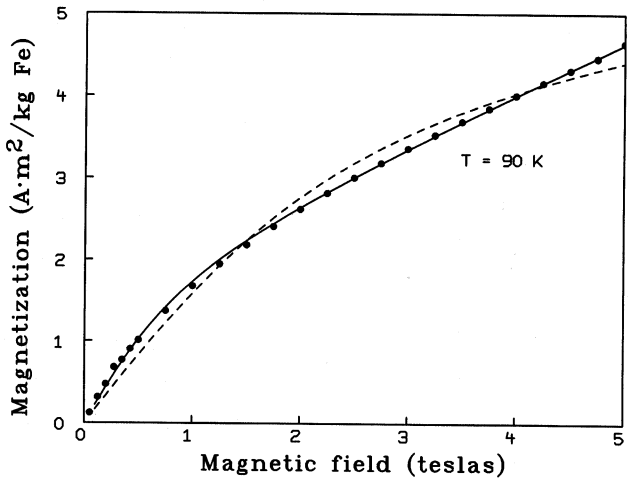

FIG. 6. A typical data set (90 K). The solid line is the fit of Fig. 4. The dashed line is the best fit if the number of SPM particles is fixed at the number of ferritin molecules.

Such a discrepancy might occur if there were perfect or near-perfect cancellation of sublattices in most ferritin cores. (This possibility was envisaged by Néel, who constructed a theory of "superantiferromagnetism" for particles with an even number of planes.) For example, if the binding of iron to complete lattices were chemically less favorable, then iron atoms would be scavenged more readily by cores with *incomplete* lattice structure, leaving other cores complete. Or, if the ions that are not AFM compensated (i.e., the ones responsible for the SPM moment) also experience the weakest exchange forces, they would become nonaligned, and hence PM, at low temperatures.

PM Component

At this point, we have no evidence (apart from the secondary curvature at low temperature) regarding whether the first term in Eq. [3] represents PM or AFM susceptibility. Let us first consider the susceptibility at 1.8 K. At this temperature, all AFM-coupled atoms are surely below the local Néel temperature, so the susceptibility can arise only from *uncoupled* "Curie PM" ions or from AFM susceptibility. Let us suppose for the moment that it is the former. Then, applying Curie's Law (with $\mu_{\text{eff}} = 5.9$ BM) to the result, we find that there are 7.93×10^{22} Curie ions per kg Fe, which is 0.7% of all Fe atoms (see Fig. 5). But this is an upper limit, so the subsequent increase to 9% at 310 K *cannot* be an increase in the number of Curie ions but must indicate, instead, a temperature dependence other than $1/T$. (In fact, N_p was allowed to vary with temperature to allow for just such a possibility.) This leaves only AFM susceptibility or C-W ions (created as the temperature rises above the local T_N) as possible explanations for the linear component of magnetization. To determine which, it will be helpful to abandon the parameter N_p and to consider, instead, the susceptibility.

Susceptibility is defined as the low-field limit of M/H. In this limit, both terms in Eq. [3] reduce to the Curie Law, and we obtain, for the component susceptibilities (m^3/kg Fe):

$$\chi_p = N_p \mu_{\text{eff}}^2 \mu_o / (3kT) \qquad [6a]$$

$$\chi_s = N_s \mu_s^2 \mu_o / (3kT) \qquad [6b]$$

where $\mu_{\text{eff}} = [(S+1)/S]^{1/2} \mu_i = 5.9$ BM for Fe^{3+}. Resultant values, calculated from the fitted parameters at each temperature of measurement, are shown in Fig. 7. Also shown is a fit of χ_p to the C-W Law,

$$\chi_p = N_{\text{cw}} \mu_{\text{eff}}^2 \mu_o / [3k(T - \theta)] \qquad [7]$$

where N_{cw} is the number of C-W ions and θ is the C-W constant. The fit is good over the entire temperature range, with $\theta = -61$ K and $N_{\text{cw}}/N = 11.5\%$, independent of temperature. The negative θ, of course, is an indication of AFM coupling.

The good C-W fit strongly suggests that χ_p arises from PM C-W Fe^{3+} ions, probably located on the core surface where the local T_N is lower. Such ions are theoretically expected, as "the molecular fields acting on internal and external atoms are surely quite different. In general, it seems logical to suppose that the external atoms are subject to a weaker molecular field than the internal atoms" (33). A PM explanation for χ_p is also consistent with the secondary curvature noted at 10 and 30 K and with the T_1 relaxometry results. AFM susceptibility,[3] on the other hand, would not exhibit a C-W temperature dependence. Even with Néel's additional superantiferromagnetism,[4] the total AFM susceptibility (at least in his simple example) decreases by only approximately 25% over the range $0 - T_N$, compared with the fourfold decrease shown in Fig. 7. This is not to say that AFM susceptibility is not present or possibly even significant at high temperatures.

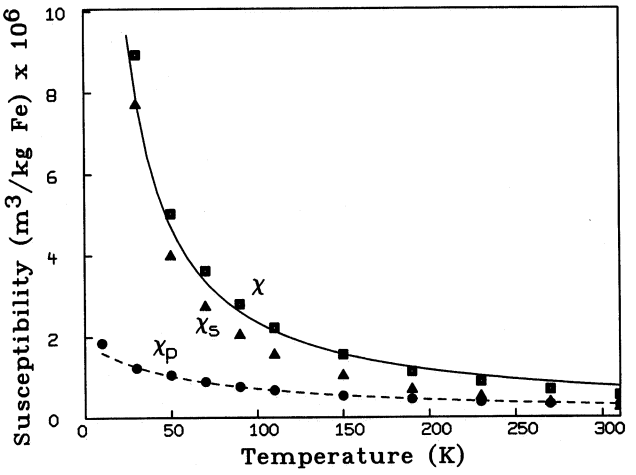

FIG. 7. Component susceptibilities χ_p (●) and χ_s (▲), and their sum χ (■), plotted versus temperature. The dashed line shows a Curie-Weiss fit to χ_p (Eq. [7]). The solid line shows an approximate Curie Law fit to the total susceptibility χ (Eq. [6a]).

There are, therefore, many reasons to conclude that χ_p is primarily PM, as we originally hypothesized. The good fit of the C-W law at temperatures as low as 30 K implies that the Néel point for these ions is no higher than 30 K. (It is not unusual for T_N to be less than $-\theta$ by a factor of 2 or more (36)). Note, however, that these C-W ions are not the same as the *ordered but uncompensated* ions that make up the SPM moment (33); they are ions that might have so contributed but, since they are *above the local* T_N, they have become *disordered and hence PM.* (A conversion from AFM order to PM disorder was also mentioned above as a possible explanation for the small number of SPM particles.)

Total Susceptibility

The total susceptibility χ is the sum of Eqs. [6a] and [6b]. The resulting values (Fig. 7) are consistent with the direct measurements, thereby demonstrating consistency in the curve-fitting procedure. As others have noted (26–29), χ approximately follows Curie's Law (Fig. 7). However, since neither component does, this is clearly coincidental. Specifically, χ_p decreases with temperature more slowly than Curie's Law (because N_p in Eq. [6a] increases with T), whereas χ_s falls more quickly (because μ_s in Eq. [6b] decreases with T). If we assume, nevertheless, that Curie's Law applies to the total, the effective Curie mo-

ment μ_c per Fe atom can be calculated from Eqs. [6a] and [6b]. The result is

$$\mu_c^2 = N_p\mu_{\text{eff}}^2/N + N_s\mu_s^2/N \quad [8]$$

This shows that μ_c can vary with *LF* and with preparation, so it is not surprising that our value (2.9 BM for *LF* = 3040) is different from values of 3.8–3.9 BM for smaller *LF* (26–29).

Comparison with Other Studies

Because there has been much confusion and contradiction in the literature, and because our results are, in some ways, different from current belief, we "retrofitted" other published data (28–32), using Eq. [3]. Following is a comparison of our results with the published analyses.

Asymptotic Analyses

In three studies (28–30), the high-field asymptote was taken as the slope of the linear component and was found to follow the C-W Law below 220–240 K, with C-W constants ranging from −200 K (28) to −239 K (30). Why the C-W behavior stopped at 220–240 K was not explained. Nevertheless, in one study (30), the linear component was attributed to AFM susceptibility, but with no explanation of the inconsistent temperature dependence. In our retrofits, we found that this component (χ_p) followed the C-W Law (at least approximately) *over the entire temperature range* for all three data sets, with C-W constants of −61 K (28), −42 K (29), and −38 K (30), thus removing an obstacle to the C-W interpretation of this term.

The other component, because of its curvature, was acknowledged to be SPM in all three studies, and in one study (28) was attributed to a "ferromagnetic component that saturates around 11000 Oe [1.1 tesla]." This was probably the best explanation at the time, since the authors were probably unaware of Néel's just-published theory of small AFM crystals (33). In a later study, the Néel theory *was* invoked (30), and a Langevin function was fitted to the low-field slopes (under the dubious assumption that the linear contribution is negligible). This yielded a SPM moment μ_s = 200 BM (30), independent of temperature. In our retrofits of that data, we found μ_s = 440–470 BM (28, 29) and 1000 BM (30) at low temperature, followed by a consistent decrease with temperature (*cf.*, Fig. 5).

Curve-Fitting Analyses

In two later studies (31, 32), the data were curve-fitted using the sum of a linear and Langevin term, as in Eq. [3], but with all three parameters permitted to vary with temperature. The linear component, which decreased with temperature in one study (32) and was relatively constant in the other (31), was attributed to *superantiferromagnetism.*[4] In our retrofits, we again found an excellent C-W dependence for this component, with C-W constants of −109 K (32) and −61 K (31).

As for the SPM moment μ_s, a magnitude of 300 BM at low temperature was found in one study (31), with a slow increase above 120 K, while a value of 300–350 BM was found in the other study (32), with little temperature dependence. In both studies, μ_s was attributed to AFM order (33). The parameter N_s was not specifically mentioned (it would be meaningless without knowing the iron concentration), but in one study (32), the coefficient of the Langevin function (M_o) was reported to decrease with temperature. However, instead of attributing this to a decrease in the number of SPM particles (since $M_o = N_s\mu_s$, and μ_s was reportedly constant), M_o was interpreted as a *second* magnetic moment *independent of* μ_s. Under this questionable interpretation, the decrease was extrapolated to zero to yield an estimate for the Néel temperature of 460 K. Our retrofitted values of μ_s agreed with the above reports (30, 31) in the low-temperature limit, after which there was a consistent *decrease*, similar to that in Fig. 5.

Alternative Explanation for SPM Temperature Dependence

The above differences in fit are evidently due to our constraint that N_s is constant. We therefore refitted our data without this constraint (not shown). The values of N_p were relatively unchanged, but μ_s now was fairly constant within the range 400–450 BM, whereas N_s/N decreased from approximately 5×10^{-5} at low temperature to 1×10^{-5} at 310 K. In other words, the temperature dependence was transferred from μ_s to N_s, consistent with ref. 32, if the parameters are reinterpreted accordingly.

The possibility that N_s varies with temperature, although surprising, could be related to the idea introduced earlier that uncanceled AFM spins responsible for the SPM moment can be converted to C-W paramagnets if the temperature rises above the local T_N, thereby reducing or removing the SPM moment. If there were a *distribution* of "surface" Néel points among the molecules, then the number of cores so converted would increase with temperature, leaving fewer SPM cores. However, this possibility raises several problems. (a) The good fit of the PM term to the simple C-W equation becomes a coincidence. (b) The "discrepancy factor" of 7 noted earlier now becomes 33 at body temperature, which is even harder to explain. (c) There does not seem to be any reason for such a smoothly varying heterogeneity of particles, whereas there is (as we saw) theoretical reason for μ_s to decrease with temperature. Nevertheless, the data seem to show a slight but consistent preference for the second fit, so the possibility should not be ruled out. In fact, the true temperature dependence could be a result of decreases in *both* N_s and μ_s with temperature.

CONCLUSIONS

Our results are different in many ways from earlier reports and have led us to suggest a new structure of the ferritin core (Fig. 8). In this model, the *interior* of the ferritin core (cross-hatched region) is AFM with a Néel temperature higher than 37°C. In some molecules (1 out of 7 for our sample), the antiferromagnetism leads to an SPM moment μ_s created by incomplete cancellation of

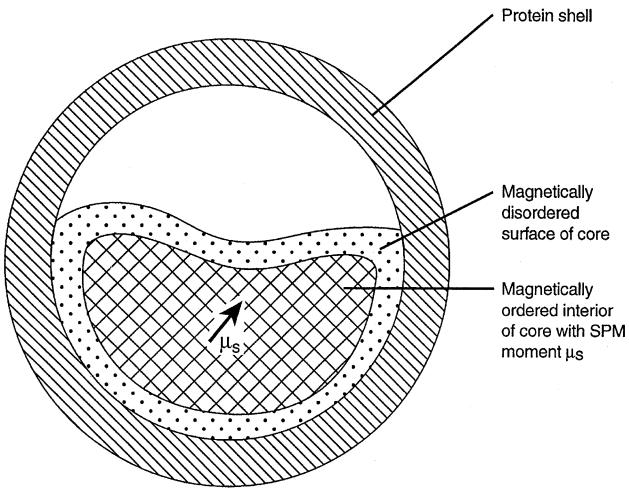

FIG. 8. Schematic drawing of a possible structure of the ferritin molecule. The core consists of two parts, both AFM. In the central region (cross-hatched), T_N is high (higher than 37°C) and the spins are antiparallel. In some molecules, this creates an SPM moment μ_s (arrow) because of a preponderance of spins in one direction or the other. In the peripheral region (dotted), the Fe^{3+} ions are also AFM coupled, but the exchange forces (or molecular fields) are much weaker and T_N is therefore very low. These ions are therefore PM and follow the C-W Law. The relative size of the two regions may change with temperature as the uncanceled spins responsible for the SPM moment find themselves above the local T_N and, hence, become PM.

sublattices (33). In other molecules, the interior region is also AFM, but the lattice structure is complete (i.e., there are an even number of AFM planes), so there is no SPM moment. This SPM moment, even if found in only a fraction of the molecules, could explain the large T_2 effect and its unusual dependence on *LF*, although the linear dependence of $1/T_2$ on field strength remains unexplained.

There is also an external core region (dotted region in Fig. 8) in which the Néel temperature is very low. Above T_N, the exchange forces are not strong enough to maintain AFM order, and these Fe^{3+} ions (11.5% in our sample) behave as C-W paramagnets.

According to this model, the total susceptibility of ferritin consists of two components with different temperature dependences which, when combined, coincidentally mimic Curie's Law. However, the Curie behavior is not exact, and the effective "Curie moment" can vary with LF and preparation.

This model, although derived mostly from the magnetometry data, is strengthened and reinforced by the agreement and consistency with the relaxometry results. Thus, the SPM moment deduced from the curvature of the magnetization curves can explain the anomalously strong T_2 relaxation, including its unusual linear dependence on *LF*. The C-W ions, inferred from the linear part of the magnetization data, can explain all aspects of the T_1 relaxation data, including the difference between T_1 and T_2 outliers.

The T_1 effect of ferritin as well as the stronger T_2 effect are observable on MRI, and a full understanding of T_1 and T_2 in ferritin solution may contribute to the development and improvement of MRI as a method of *in vivo* iron measurement.

ACKNOWLEDGMENTS

The authors thank Olga Zak for her advice and help in the art of ferritin preparation; David Gordon and Jacob Schroeder for their untiring efforts in the chemical laboratory; Vu Tran, Phuc Nguyen, and Kimberly Do for performing many repetitive T_1/T_2 measurements; and Janusz Karaszewski for help in curve-fitting the magnetometry data. We especially thank Erica Bauminger, Richard Frankel, and Trevor Douglas for helpful discussions and valuable suggestions.

REFERENCES

1. K. L. Taft, G. C. Papaefthymiou, S. J. Lippard, A mixed-valent poly-iron oxo complex that models the biomineralization of the ferritin core. *Science* **259,** 1302–1305 (1993).
2. S. Gider, D. D. Awschalom, T. Douglas, S. Mann, M. Chaparala, Classical and quantum magnetic phenomena in natural and artifical ferritin proteins. *Science* **268,** 77–80 (1995).
3. A. Treffry, Z. Zhao, M. A. Quail, J. R. Guest, P. M. Harrison, Dinuclear center of ferritin: studies of iron binding and oxidation show differences in the two iron sites. *Biochemistry* **36,** 432–441 (1997).
4. S. Hilty, B. Webb, R. B. Frankel, G. D. Watt, Iron core formation in horse spleen ferritin: magnetic susceptibility, pH, and compositional studies. *J. Inorg. Biochem.* **56,** 173–185 (1994).
5. R. B. Frankel, G. C. Papaefthymiou, G. D. Watt, Variation of superparamagnetic properties with iron loading in mammalian ferritin. *Hyperfine Interactions* **66,** 71–82 (1991).
6. E. R. Bauminger, P. M. Harrison, D. Hechel, I. Nowik, A. Treffry, Mössbauer spectroscopic investigation of structure-function relations in ferritin. *Biochim. Biophys. Acta* **1118,** 48–58 (1991).
7. D. D. Awschalom, D. P. DiVincenzo, J. F. Smyth, Macroscopic quantum effects in nanometer-scale magnets. *Science* **258,** 414–421 (1992).
8. J. Vymazal, M. Hajek, N. Patronas, J. N. Giedd, J. W. M. Bulte, R. A. Brooks, The quantitative relation between T1- and T2-weighted MRI of normal gray matter and iron concentration. *J. Magn. Reson. Imaging* **5,** 554–560 (1995).
9. G. Bartzokis, S. R. Marder, Magnetic resonance imaging evaluation of brain iron levels. *Biol. Psychiatry* **38,** 133–135 (1995).
10. R. Engelhardt, J. H. Langkowski, R. Fischer, P. Nielsen, H. Kooijman, H. C. Heinrich, E. Bücheler, Liver iron quantification: studies in aqueous iron solutions, iron-overloaded rats, and patients with hereditary hemochromatosis. *Magn. Reson. Imaging* **12,** 999–1007 (1994).
11. F. C. Meldrum, B. R. Heywood, S. Mann, Magnetoferritin: in vitro synthesis of a novel magnetic protein. *Science* **257,** 522–523 (1992).
12. J. W. M. Bulte, T. Douglas, S. Mann, J. Vymazal, P. G. Laughlin, J. A. Frank, Initial assessment of magnetoferritin biokinetics and proton relaxation enhancement in rats. *Acad. Radiol.* **2,** 871–878 (1995).
13. J. F. Hainfeld, Uranium-loaded apoferritin with antibodies attached: molecular design for uranium neutron-capture therapy. *Proc. Natl. Acad. Sci. U S A* **89,** 11064–11068 (1992).
14. T. Douglas, D. P. E. Dickson, S. Betteridge, J. Charnock, C. D. Garner, S. Mann, Synthesis and structure of an iron(III) sulfide-ferritin bioinorganic nanocomposite. *Science* **269,** 54–57 (1995).
15. J. Vymazal, R. A. Brooks, N. Patronas, M. Hajek, J. W. M. Bulte, G. Di Chiro, Magnetic resonance imaging of brain iron in health and disease. *J. Neurol. Sci.* **134(Suppl),** 19–26 (1995).
16. O. H. Lowry, N. J. Rosebrough, L. Farr, R. J. Randall, Protein measurement with the Folin Phenol reagent. *J. Biol. Chem.* **193,** 267–275 (1951).
17. S. H. Koenig, R. D. I. I. I. Brown, J. F. Gibson, R. J. Ward, T. J. Peters, Relaxometry of ferritin solutions and the influence of the Fe^{3+} core ions. *Magn. Reson. Med.* **3,** 755–767 (1986).
18. J. Vymazal, O. Zak, J. W. M. Bulte, P. Aisen, R. A. Brooks, T_1 and T_2 of ferritin solutions: effect of loading factor. *Magn. Reson. Med.* **36,** 61–65 (1996).
19. J. Vymazal, R. A. Brooks, O. Zak, C. McRill, C. Shen, G. Di Chiro, T_1

and T_2 of ferritin at different field strengths: effect on MRI. *Magn. Reson. Med.* **27,** 368–374 (1992).
20. Z. Gottesfeld, M. Neeman, Ferritin effect on the transverse relaxation of water: NMR microscopy at 9.4 T. *Magn. Reson. Med.* **35,** 514–520 (1996).
21. A. Roch, R. N. Muller, Longitudinal relaxation of water protons in colloidal suspensions of superparamagnetic crystals, *in* "Proc., SMRM, 11th Annual Meeting, Berlin, 1992," p. 1447.
22. S. H. Koenig, K. E. Kellar, Theory of $1/T_1$ and $1/T_2$ NMRD profiles of solutions of magnetic nanoparticles. *Magn. Reson. Med.* **34,** 227–233 (1995).
23. S. H. Koenig, R. D. Brown III, Relaxation of solvent protons by paramagnetic ions and its dependence on magnetic field and chemical environment: implications for NMR imaging. *Magn. Reson. Med.* **1,** 478–495 (1984).
24. C. C. Lester, R. G. Bryant, Magnetically coupled paramagnetic relaxation agents. *Magn. Reson. Med.* **24,** 236–242 (1992).
25. J. W. M. Bulte, J. Vymazal, R. A. Brooks, C. Pierpaoli, J. A. Frank, Frequency dependence of NMR relaxation times: II. Iron oxides. *J. Magn. Reson. Imaging* **3,** 641–648 (1993).
26. L. Michaelis, C. D. Coryell, S. Granick, The magnetic properties of ferritin and some other colloidal ferric compounds. *J. Biol. Chem.* **148,** 463–480 (1943).
27. G. Schoffa, Der antiferromagnetismus des ferritins bei Messungen der magnetischen suszeptibilität im temperaturbereich von 4.2 bis 300°K. *Z. Naturforschg.* **20,** 167–172 (1965).
28. A. Blaise, J. Chappert, J. -L. Girardet, Observation par mesures magnéetiques et effet Mössbauer d'un antiferromagnétisme de grains fins dans la ferritine. *Comptes Rendus Acad. Sci.* **261,** 2310–2313 (1965).
29. A. Blaise, J. Féron, J. -L. Girardet, J. -J. Lawrence, Contribution à l'étude des propriétés magnétiques de la ferritine. *Comptes Rendus Acad. Sci.* **265,** 1077–1080 (1967).
30. M. -E. Y. Mohie-Eldin, R. B. Frankel, L. Gunther, A comparison of the magnetic properties of polysaccharide iron complex (PIC) and ferritin. *J. Magn. Magn. Mater.* **135,** 65–81 (1994).
31. S. H. Kilcoyne, R. Cywinski. Ferritin —a model superparamagnet. *J. Magn. Magn. Mater.* **140,** 1466–1467 (1995).
32. S. A. Makhlouf, F. T. Parker, A. E. Berkowitz, Magnetic hysteresis anomalies in ferritin. *Phys. Rev. B* **55,** R14717–720 (1997).
33. L. Néel, Superparamagnétisme de grains très fins antiferromagnétiques. *Comptes Rendus Acad. Sci.* **252,** 4075–4080 (1961). [Translated in "Selected Works of Louis Néel" (N. Kurti, Ed.), pp. 107–110, Gordon and Breach, New York, 1988.]
34. A. Blaise, J. L. Girardet, Ferritin iron core: high field magnetization and Néel temperature, *in* "Proc., International Conference on Magnetism ICM-73, Moscow, 1974," pp. 280–281.
35. E. R. Bauminger, I. Nowik, Magnetism in plant and mammalian ferritin. *Hyperfine Interactions* **50,** 484–498 (1989).
36. C. Kittel, "Introduction to Solid State Physics," 3rd ed., p. 484, John Wiley & Sons, New York, 1966.
37. L. Néel, Superantiferromagnétisme dans les grains très fins. *Comptes Rendus Acad. Sci.* **253,** 203–208 (1961). [Translated in "Selected Works of Louis Néel" (N. Kurti, Ed.), pp. 114–117, Gordon and Breach, New York, 1988.]
38. L. Néel, Sur le calcul de la susceptibilité additionnelle superantiferromagnétique des grains fins et sa variation thermique. *Comptes Rendus Acad. Sci.* **253,** 1286–1291 (1961). [Translated in "Selected Works of Louis Néel" (N. Kurti, Ed.), pp. 118–121, Gordon and Breach, New York, 1988.]